RSC Advances

PAPER

View Article Online
View Journal | View Issue

Cite this: *RSC Adv.*, 2018, **8**, 13806

Controlled self-assembly of glycoprotein complex in snail mucus from lubricating liquid to elastic fiber

Tianyi Zhong,[a] Liu Min,[a] Zhiyuan Wang,[b] Feng Zhang[c] and Baoqi Zuo *[a]

Received 14th February 2018
Accepted 22nd March 2018

DOI: 10.1039/c8ra01439f

rsc.li/rsc-advances

The pedal mucus secreted by many gastropod mollusks, such as terrestrial snails and slugs, plays crucial roles in locomotion, osmoregulation, reproduction, and repulsing predators. In this report, we presented an intriguing example that terrestrial snail can utilize the self-assembly of glycoprotein complex in secreted mucus at the nanoscale to enhance adhesive force on smooth plates. With increasing crawling angle, the structural transformation of pedal mucus was found to involve at least four distinct stages: assembly of nanoparticles, aggregation into microspheres, formation of gels and solidification into fibers. These forming processes were mainly attributed to the unique combination of amino acid composition and chemistry in secreted glycoprotein coupled with the calcium carbonate regulation in pedal gland. Most importantly, we were inspired by these forming process to obtain a novel biomimetic fiber with good extensibility and elasticity from extracted pedal mucus for potential biomedical application.

Introduction

In nature many creatures employ distinctive behavioral strategies combined with well-designed adhesives for locomotion, defense, and prey capture.[1–5] Just like spiders employ multiple kinds of custom-made protein fibers with unique elasticity to catch elusive prey.[6] Another intriguing example is provided by terrestrial snails, which rely on a thin layer of secreted mucus from pedal gland for adhesive locomotion.[7] This locomotion is driven by a succession of periodic muscular waves (alternate contraction and relaxation) moving along the ventral of the foot.[8] Applied stresses generated by these waves is coupled to the substratum by this pedal mucus. It is generally believed that the mucus is a physically crosslinked gel containing approximately 90–99% weight of water.[9] The fundamental constituent is a mucin-like glycoprotein complex, dominating its viscoelasticity that allow the snail to crawl onto vertical and even inverted plates.[10] The pedal mucus has distinctive yield–heal properties: it can break into a viscous liquid at high shear stresses enabling snail to glide forward over a fluid layer. By contrast, it will recover into a viscoelastic solid at low shear stresses holding snail to the substrate.

In the last years many researchers have attempted to capture the key features of pedal mucus to understand and replicate snail's capabilities.[11–13] They have established different material and mechanical models for the development of bioinspired adhesives or innovative robotic devices. However, snail can secrete different formulations of mucus for the complex environment, ranging from a slippery lubricant employed during locomotion to powerful glue used for adhesion over long time.[14] It remains unknown how microstructure of this glycoprotein-based mucus contribute to its adhesive locomotion.

In present study, we noted that snail could take advantages of both the elasticity and the extensibility of fibers, clinging itself onto the inverted smooth plate. To further explore this phenomenon, we left the snail to crawl on the smooth plate with different angles in order to obtain corresponding adhesive mucus. Our focus was on the mechanism of structural transformation of snail mucus from lubricating fluid into fiber, aiming to obtain this novel biomimetic fiber from extracted pedal mucus.

Experimental

Materials

Terrestrial snail (*Achatina fulica*, white jade) was used in present study. Prior to the experiments, snails were cultured in the laboratory at 25 °C, 65% RH for about 24 h to acclimate to the laboratory environment. Snails were first allowed to prevent the mulch and other debris on their foot. Then they were left to crawl on the smooth silicon wafer to collect pedal mucus. Until snails had travelled for one minute, the deposited mucus simples were directly put into liquid nitrogen for quick-frozen to avoid structural change, then stored at −40 °C for 12 hours before lyophilization. The main drying was performed at −40 °C, 0.1 mbar (vacuum) for 12 hours using a lyophilizer (Marin Christ ALPHA 1-2 LD). The final drying was performed from −40 °C to 25 °C within 2 hour, 0.1 mbar. The hydrated

[a]*College of Textile and Clothing Engineering, Soochow University, National Engineering Laboratory for Modern Silk, Suzhou Jiangsu, 215000, PR China. E-mail: bqzuo@suda.edu.cn; Fax: +86-0512-67246786; Tel: +86-0512-67061157*

[b]*Suzhou Sirnaomics Pharmaceuticals Ltd., Biobay, Suzhou, China*

[c]*Medical College of Soochow University, Jiangsu Province Key Laboratory of Stem Cell Research, Suzhou Jiangsu, 215000, PR China*

mucus samples were gathered by scraping the deposited mucus with a razor blade behind the crawling snail on different angles of smooth plates.

Characterization

Morphological structure of snail mucus. Morphology of lyophilized mucus simples was observed using a field emission scanning electronic microscopy (SEM, Hitachi S-480). The lyophilized samples were sputter coated with gold prior to imaging. Morphology of hydrated mucus samples was observed using an atomic force microscope (AFM, VECCO multimode). The mucus samples were diluted to below 1 mg mL^{-1}, then dripped 5 μL on the mica plate for observation.

Composition of snail mucus. Elemental analysis of lyophilized sample was carried out on the metal specimen using the energy dispersive spectrometer (EDS, Oxford SwiftED3000) combined with scanning electron microscope (Hitachi TM3030). The weight loss of lyophilized sample in N_2 with a heating rate of 10 °C min^{-1} was measured by a thermogravimetric analyzer (TGA, Mettler Toledo Thermal). Lyophilized sample was pretreated with tiny boiling hydrochloric acid for decomposition and purification, then measured by using an amino acid analyzer (Hitachi L8900) to obtain the amino acid composition.

Rheological measurements. Rheological frequency and strain sweeps were performed using a strain-controlled rheometer (TA AR2000) with 40 mm-diameter stainless steel parallel plate geometries at 0.5 mm measuring gap distance. Strain sweep measurements were performed from 1% to 1000%. Frequency sweeps were collected over a wide frequency range from 1 to 100 rad s^{-1}.

Particle size and zeta potential. The average particle size and zeta potential were obtained using an affordable molecular/particle size and zeta potential analyzer (Malvern Nano ZS90). The calcium carbonate (superfine powder, average particle size: 50–80 nm) was used to simulate the calcium component in pedal mucus. Before mixing with pedal mucus, calcium carbonate was added in purified water then stirred 30 minutes under ultrasonic vibration for dispersion.

Structural and mechanical properties. The extracted pedal mucus was diluted to 1–10 mg mL^{-1} solution, and centrifuged to remove impurities. The spinning solution of extracted mucus was drawn at different speeds and solidified into fiber at air. Fourier transform infrared spectroscopy was obtained using a Magna spectrometer (FTIR, NicoLET5700) in the spectral region of 400–4000 cm^{-1}, the powdered fiber was pressed into potassium bromide pellets prior to data collection. The mechanical data of force-drawn fibers were obtained using a universal testing machine (Instron3365).

Results and discussion

Structural transformation of snail mucus

Pedal mucus from the terrestrial snail *Achatina fulica* (white jade) was measured in the entire research process (Fig. 1A). The field emission scanning electronic microscopy (SEM) images in Fig. 1B illustrated the morphological structure of mucus sample from snail crawling on an inverted silicon wafer. Dozens of fibers with diameters of 10.5 ± 0.5 μm entwined together on the smooth plate. The zoomed-in images showed these were many small micro-globules on the fiber plate, which were further assembled by many nanoparticles with diameters of tens of nanometers. This special fiber-structure of mucus was significantly different from the gel-structure previous reported. We initially speculated that the snail also relies on the elasticity of these fibers to cling on the smooth plate. In order to explore this

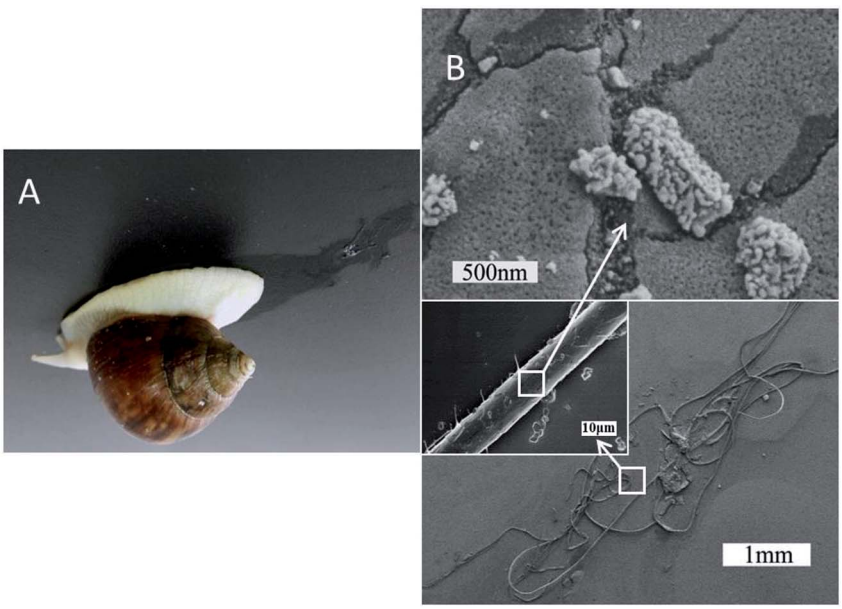

Fig. 1 SEM images of fiber-structure consisting of many nanoparticles (B) collected from terrestrial snail crawling on the inverted plate (A).

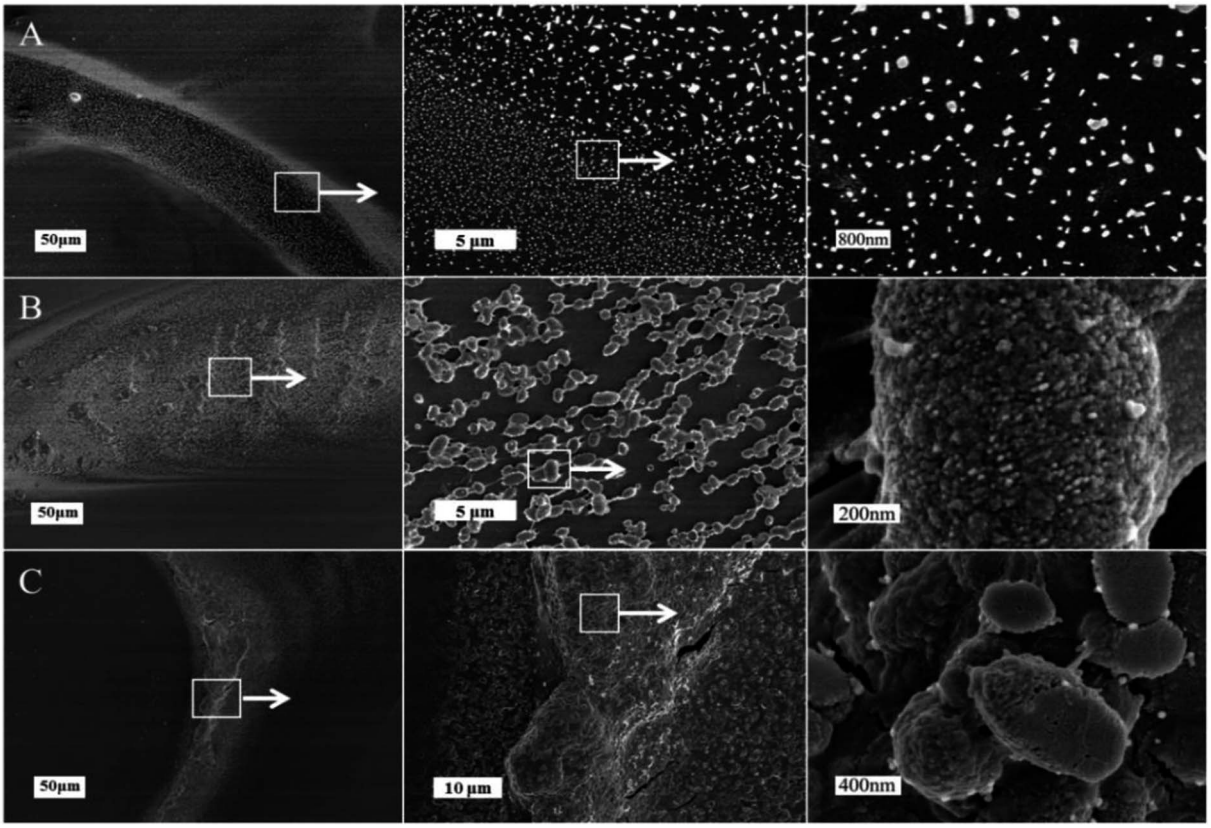

Fig. 2 SEM images of different mucus samples collected from snail crawling on the horizontal (A), 45° inclined (B) and vertical smooth plates (C) respectively.

phenomenon, mucus samples from snail crawling on the smooth plate with different angles were measured as following.

Fig. 2 illustrated the morphological structure of mucus sample from snail crawling on different angles of silicon wafer. When snail crawled on the horizontal smooth plate, there was an obvious mucus trail consisting of many nanoparticles with diameters of 50–200 nm (Fig. 2A). Images of mucus solution from atomic force microscopy (AFM) also showed there were many globular nanoparticles with diameters of tens of nanometers distributed uniformly on mica plate (Fig. 3A). To further confirm this process, rheological frequency and strain sweeps were used to monitor the rheological behaviors of mucus samples (Fig. 4A). The sample collected from snail crawling on the horizontal plate essentially behaved as a Newtonian liquid: the shear modulus displayed weak frequency-dependent between 0.01–1 Pa, and loss modulus (G″) higher than storage modulus (G′) at most measured points. The strain sweeps also showed the oscillatory stress of this mucus was approximate linear proportional to the local strain rate. In fact, the snail did not need sticky mucus on the horizontal plate to fix its body, but rather lubricating mucus to help its crawling. When snail crawled on a 45° inclined smooth plate, SEM images of mucus trail showed many spheres with micrometer scale, in the size range several hundreds of nanometers to several micrometers (Fig. 3B). Interestingly, these larger microspheres were assembled from the small nanoparticles with diameters of tens of nanometers. These microspheres gathered together slightly, suggesting this mucus was more like viscous fluid. AFM images illustrated the agglomeration trend of these microspheres. Moreover, results from rheological measurements confirmed that this sample behaved as a low-viscosity fluid: the shear modulus displayed weak frequency-dependent between 1–10 Pa, and G′ higher than G″ at all observed time. The property of shear thickening at low strain rate and shear thinning when the strain rate surpass the critical point was manifested by the strain sweep measurement. When snail crawled on a vertical smooth plate, the mucus exhibited apparent mucus trail with gel-like structure (Fig. 3C). The zoomed-in images further showed this gel-structure was assembled from a lot of microspheres with diameter of micrometers. The coalescence of microspheres was more compact suggesting a highly interconnected structure. AFM images also illustrated the more obvious gel-film structure. This mucus sample showed apparent gel-like behaviors with higher shear modulus: G′ higher than G″ within the observed time, shear thickening at first and shear thinning after critical strain rate.

Self-assembly mechanism

Obviously, snail could precisely control the structure of secreted mucus when crawled on different angles of smooth plates. Based on these morphological results, small nanoparticles with sizes of tens of nanometers appeared to be the basic assembly

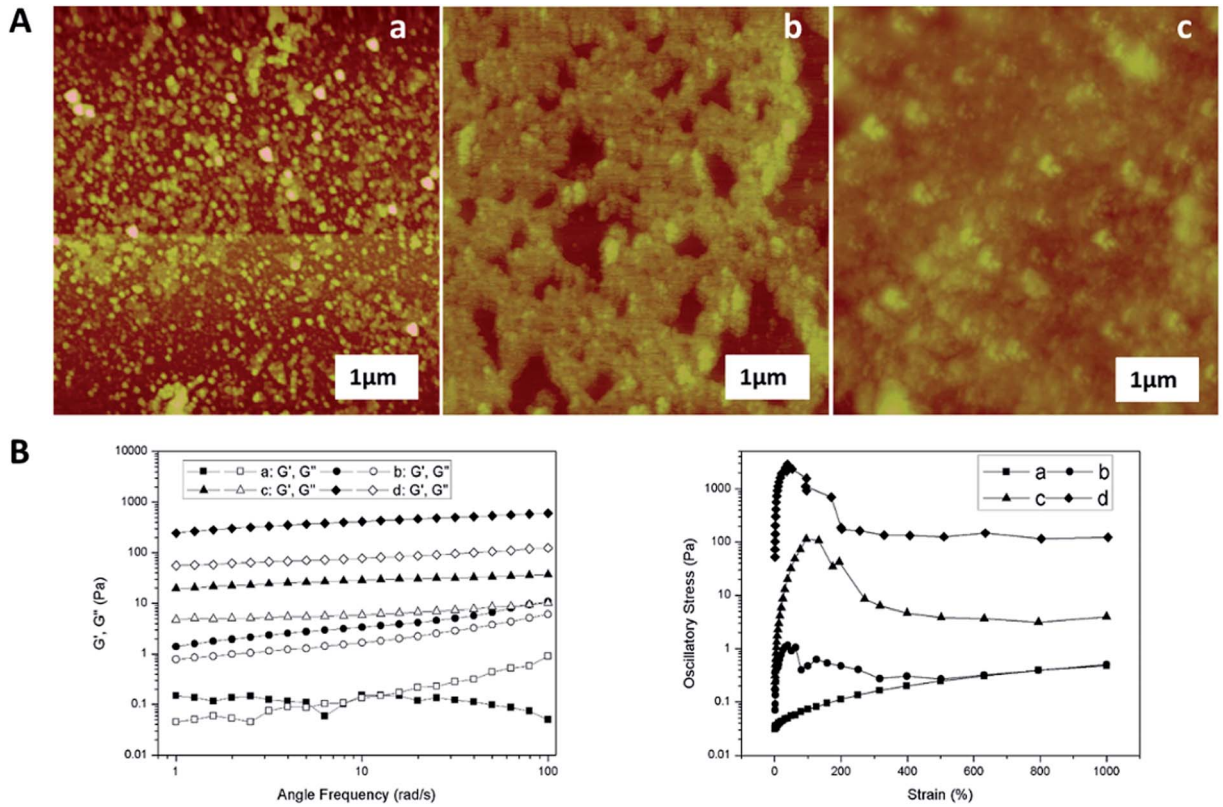

Fig. 3 (A) AFM images of mucus solution collected from snail crawling on the horizontal (a), 45° inclined (b), and vertical plates (c) respectively. (B) Rheology frequency and strain sweeps of mucus samples collected from snail crawling on the horizontal (a), 45° inclined (b), vertical (c), and inverted (d) plates respectively.

component. A number of studies have reported the glycoprotein complexes always condense into secretory granule and expand by hydration during or after exocytosis.[15] The hydrated glycoprotein granule will be swelled into nanoparticle by hydrophilic/hydrophobic interaction with leaving internal hydrophobic blocks and external hydrophilic blocks to promote

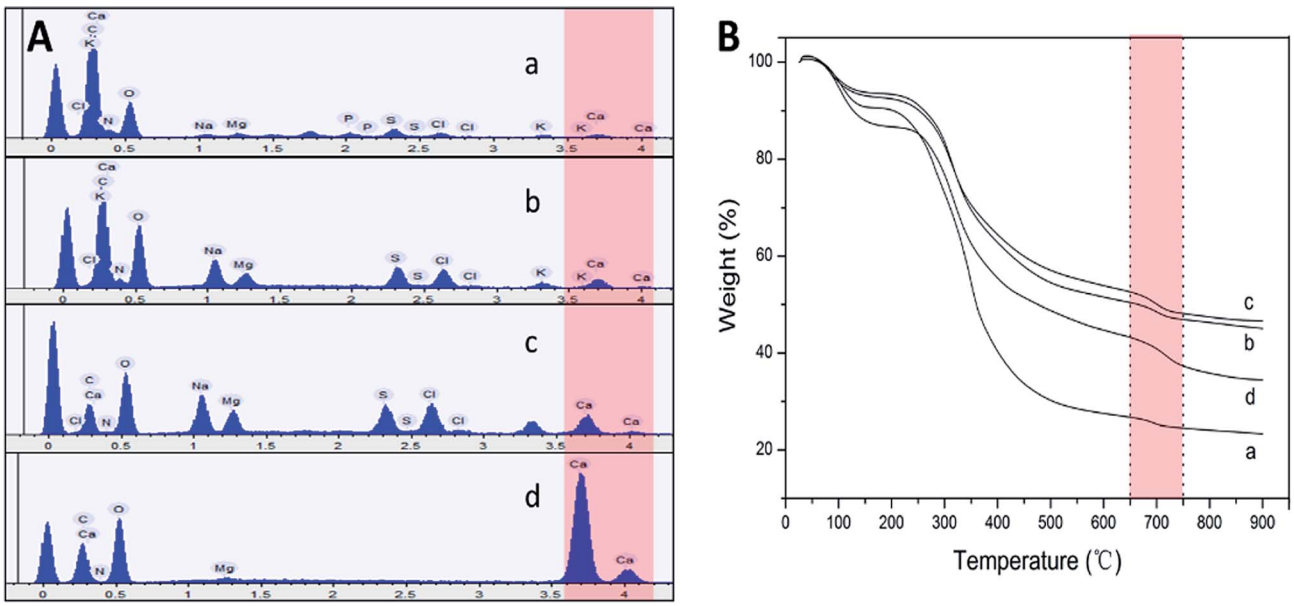

Fig. 4 (A) EDS results of the mucus collected from snail crawling on the horizontal (a), 45° inclined (b), vertical (c), and inverted (d) plates respectively. (B) TGA results collected from the same samples as in EDS.

solubility in water.[16] In terrestrial and freshwater snails, the secreted mucus from pedal gland is always accompanied with the calcium carbonate metabolism.[17] Granules of glycoprotein-calcium carbonate are enriched in the goblet cell of snail's foot that has been identified.[18,19] As a weak alkaline salt, calcium carbonate plays a very important role as a nucleator in the structural transformation of mucus which would react electrostatically with the anionic glycoprotein.[20] Results from amino acid analyzer showed that the amino acid composition of this protein-rich mucus was dominated by the high proportion of hydrophilic amino acids like glutamic acid and aspartic acid (Fig. 5A). Although the amino acid composition of glycoprotein complexes under different conditions was slightly different, but the main component was the same. Results from energy dispersive spectrometer (EDS) analysis showed that the content of calcium element in secreted mucus was increasing constantly from 0.56% to 13.45% during the structural transition (Fig. 4A). Moreover, thermogravimetric analysis (TGA) was used to characterize the weight contents of calcium component in mucus (Fig. 4B). The thermal decomposition peaks of calcium carbonate between 650–750 °C showed that the weight loss of mucus samples were 2.19%, 3.43%, 4.41%, and 5.93% respectively.[21] Thus calculated weight content of calcium carbonate was also increasing constantly from 4.98% to 13.48% during the four structural transformation stages.

To further confirm this process, we measured the particle size and zeta potential of the diluted mucus in purified water and 0.1 M PBS (pH = 7.4, phosphate buffer solution) with different ratios of calcium carbonate respectively (Fig. 5B). In purified water, the average particle size of diluted mucus increased obviously from 200 nm to 1244 nm with the increasing concentration of calcium carbonate, and zeta potential also increased from −35.0 mV to −16.3 mV. But in 0.1 M PBS, there was little change in average particle size and zeta potential with the increasing concentration of calcium carbonate, because the charge effects between calcium carbonate and glycoprotein was shielded.[9,13] These results also suggested that the agglomeration of nanoparticles was caused by the calcium carbonate. When snail crawled on an inclined plate, it needed to overcome the influence of gravity. Therefore, more calcium carbonate began to act as a core that small nanoparticles assembled into larger microspheres in mucus at this point. This structural transformation would improve the viscosity of mucus facilitating adhesive locomotion. As the concentration of glycoprotein complexes increased, intermicelle interactions increased, leading to coalescence and the formation of globules and gels. The mucus gel served as glue to offer higher stiffness and viscosity that would conduce to adhesive locomotion on a vertical plate. It has been known that the pedal mucus from terrestrial gastropods exhibits special yield stress, which structure breaks at high shear stresses facilitating forward movement on fluid layer, and recovers as a solid-like layer at relatively low applied stress resisting backward movement.[22] This highly interconnected gel-structure consisting of larger microspheres would be better to explain the yield-heal feature.

Biomimetic elastic fiber

The formation of silk as a natural protein fiber involves shear and extrusion stress acting on the spinning solution, resulting in the conformation transition of macromolecule to crystallize.[23,24] The fiber formation of secreted mucus occurred during the relatively short time after the snail clinging on an inverted plate. This mucus behaved as a viscoelastic fluid with the highest viscosity in the rheological measurements whose G′ is nearly 10 times higher than G″. Similar to a liquid crystal spinning process, elongational flow oriented the gel-like mucus to a sol state with snail locomotion, following by solidification into fiber.[25] Therefore, we examined the mechanical properties of force-drawn fibers from the mucus solution which was artificially extracted from snail (Fig. 6A). When the rate of drawing speed was too slow (4 mm s^{-1}), the surface of formed fiber was irregular, composing of many granules in a wide range of sizes (Fig. 6C). Fast spinning at 16 mm s^{-1} showed a highest breaking elongation of nearly 40% for the formed fiber with the

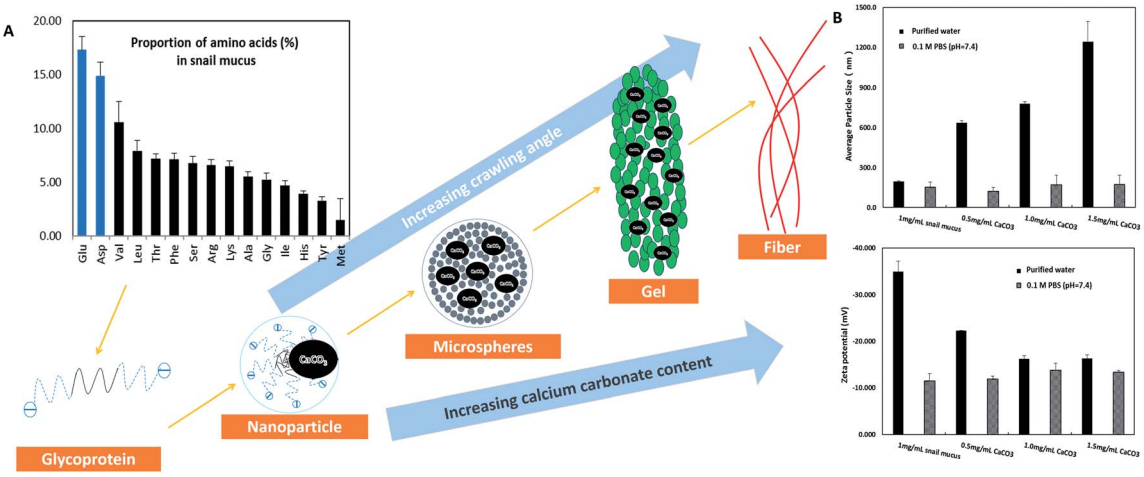

Fig. 5 Model of the structural transformation of secreted mucus. (A) Molecular pattern of snail glycoprotein was based on the amino acid composition results. (B) Results of average particle size and zeta potential collected from the diluted mucus (1 mg mL^{-1}) in purified water and 0.1 M PBS (pH = 7.4) containing 0, 0.5, 1, 1.5 mg mL^{-1} additional calcium carbonate respectively.

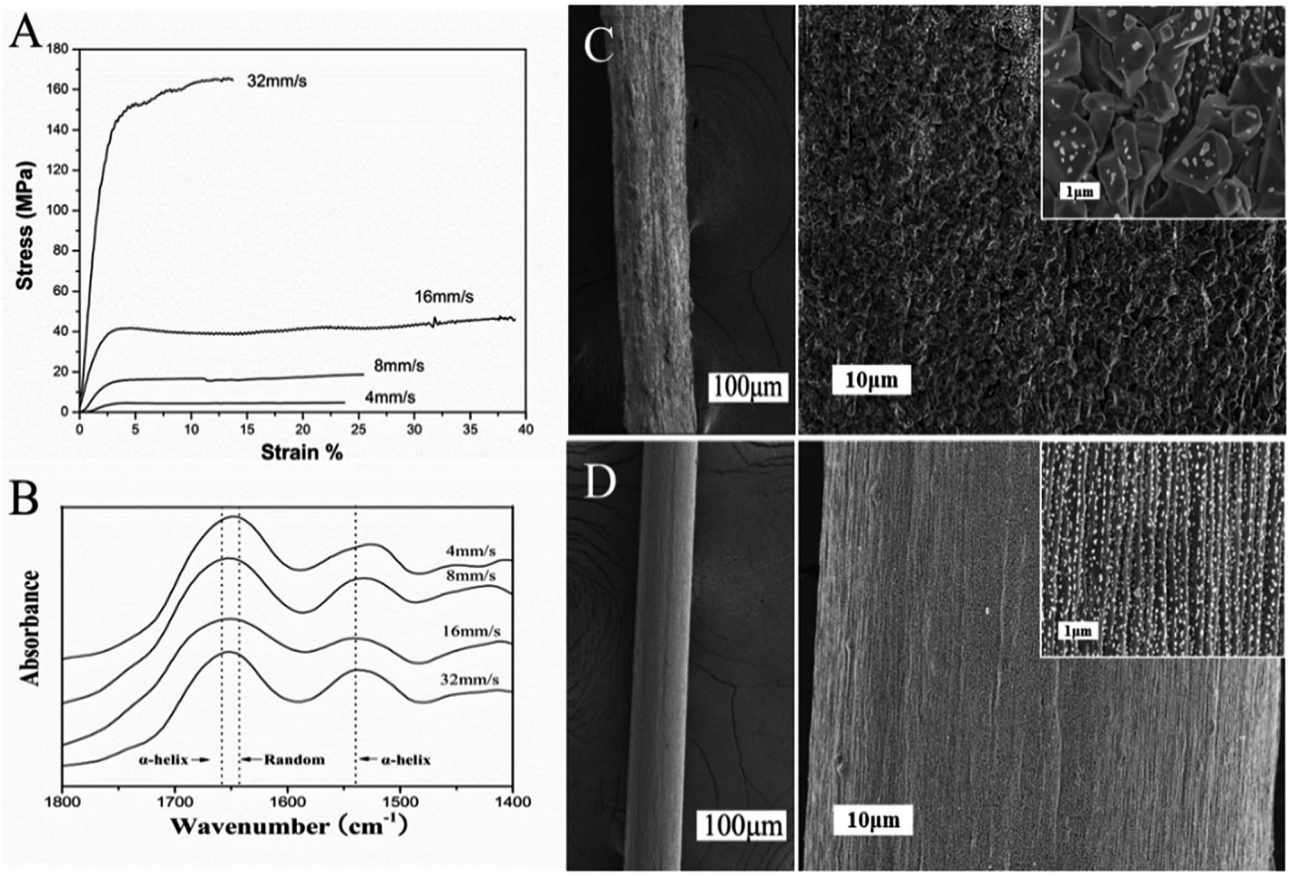

Fig. 6 Mechanical results collected from force-drawn fibers which were spun out at different drawing speeds from the extracted mucus solution (A). FTIR results collected from the force-drawn fibers (B). SEM images of the force-drawn fiber spun out at 4 mm s^{-1} (C) and 16 mm s^{-1} drawing speed (D).

smoothest surface and uniform diameter. The SEM images in Fig. 6D showed this fiber presented an obvious orientation structure. At even greater spinning speeds of 32 mm s^{-1}, the tensile strength of fibers increased to nearly 165 MPa, but there was a loss of extensibility. Moreover, we employed Fourier transform infrared spectroscopy (FTIR) to monitor the conformation of glycoprotein in force-drawn fibers (Fig. 6B). The spectrum showed the peaks at amide I and II bands were mainly attributed to α-helix and random coil structures, providing useful information on the crystalline structure of fibers from snail mucus.[26] The uniform orientation and α-helix crystalline structure of protein fiber always results in better tensile elongation and strength. For many snails, the high metabolic cost of adhesive locomotion limited their crawling speed. These extensible glycoprotein fibers could be stretched like an elastic rubber band, making the snail to crawl long enough at slow rate. But also the resilience force would enhance with increasing extension rate, retaining the snails on the inverted smooth plate without falling off.

Conclusion

In this work, we found that terrestrial snail could ingeniously employ various structures of secreted mucus to enhance adhesive forces for crawling on different angles of smooth plates, suggesting a new view of the adhesion strategy in gastropod mollusks. As secretion of mucus accompanied by calcium carbonate regulation, the self-assembly of glycoprotein complex in secreted mucus from lubricating liquid to elastic fiber indicated an insightful direction of designing adhesives and fibers. Our findings also described a natural protein fiber with nearly 40% breaking elongation and 165 MPa tensile strength which have been neglected. Unlike the spider viscid silk was hard to gather and use, this fiber could be spun out easily under regulated conditions from extracted pedal mucus which could be commercially obtained. When combine with currently used of snail mucus in human cosmetics and in the treatment of wounds and other skin lesions, the potential application of this fiber in medicine is broad.

Conflicts of interest

There are no conflicts to declare.

Acknowledgements

This work was supported by the Second Phase of Jiangsu Universities' Distinctive Discipline Development Program for Textile Science and Engineering of Soochow University, the Graduate Student Innovation Project of Jiangsu Province

(KYZZ15_0327), the National Natural Science Foundation of China (81271723), General University Natural Science Research Project of Jiangsu Province (17KJB540004) and the Natural Science Foundation of Jiangsu Province (BK20141207).

References

1 J. H. Waite and M. L. Waite, *Science*, 1981, **212**, 1038–1040.
2 A. M. Smith, T. J. Quick and R. S. Peter, *Biol. Bull.*, 1999, **196**, 34–44.
3 H. Lee, B. P. Lee and P. B. Messersmith, *Nature*, 2007, **448**, 338–341.
4 V. Sahni, T. Miyoshi, K. Chen, D. Jain, S. J. Blamires, T. A. Blackledge and A. Dhinojwala, *Biomacromolecules*, 2014, **15**, 1225–1232.
5 M. Rahimnejad and W. Zhong, *RSC Adv.*, 2017, **7**, 47380–47396.
6 V. Sahni, T. A. Blackledge and A. Dhinojwala, *J Adhes.*, 2006, **87**, 595–614.
7 M. Denny, *Nature*, 2000, **285**, 160–161.
8 B. Chan, N. J. Balmforth and A. E. Hosoi, *Phys. Fluids*, 2005, **17**, 113101.
9 J. M. Pawlicki, L. B. Pease, C. M. Pierce, T. P. Startz, Y. Zhang and A. M. Smith, *J. Exp. Biol.*, 2004, **207**, 1127–1135.
10 E. Lauga and A. E. Hosoi, *Phys. Fluids*, 2006, **18**, 113102.
11 T. Nakamura and K. Satoh, *Industrial Robot: An International Journal*, 2008, **35**, 206–210.
12 M. Iwamoto, D. Ueyama and R. Kobayashi, *J. Theor. Biol.*, 2014, **353**, 133–141.
13 J. Newar and A. Ghatak, *Langmuir*, 2015, **31**, 12155–12160.
14 T. P. Ng, S. H. Saltin, M. S. Davies, K. Johannesson, R. Stafford and G. A. Williams, *Biological Reviews*, 2013, **88**, 683–700.
15 A. M. Smith and M. C. Morin, *Biol. Bull.*, 2002, **203**, 338–346.
16 P. Verdugo, I. Deyrup-Olsen, M. Aitken, M. Villalon and D. Johnson, *J. Dent. Res.*, 1987, **66**, 506–508.
17 A. Beeby and L. Richmond, *J. Molluscan Stud*, 2007, **73**, 105–112.
18 M. S. Davies and S. J. Hutchinson, *Hydrobiologia*, 1995, **309**, 117–121.
19 S. Greistorfer, W. Klepal, N. Cyran, A. Gugumuck, L. Rudoll, J. Suppan and J. V. Byern, *Zoology*, 2017, **122**, 126–138.
20 P. G. Vekilov, *Nanoscale*, 2010, **2**, 2346–2357.
21 R. Viswanathan, T. S. L. Narasimhan and S. Nalini, *J. Chem. Eng. Data*, 2010, **55**, 3779–3785.
22 R. H. Ewoldt, C. Clasen, A. E. Hosoi and G. H. Mckinley, *Soft Matter*, 2007, **3**, 634–643.
23 F. Vollrath and D. P. Knight, *Nature*, 2001, **410**, 541–548.
24 L. Liu, X. Yang, H. Yu, C. Ma and J. Yao, *RSC Adv.*, 2014, **4**, 14304–14313.
25 Z. Shao and F. Vollrath, *Nature*, 2002, **418**, 741.
26 G. G. Leisk, T. J. Lo, T. Yucel, Q. Lu and D. L. Kaplan, *Adv. Mater.*, 2010, **22**, 711–715.

